



A Bayesian approach to degradation-based burn-in optimization for display products exhibiting two-phase degradation patterns



Tao Yuan^a, Suk Joo Bae^b, Xiaoyan Zhu^c

^a Department of Industrial and Systems Engineering, Ohio University, Athens, OH 45701, USA

^b Department of Industrial Engineering, Hanyang University, Seoul, South Korea

^c School of Economics and Management, University of Chinese Academy of Sciences, Beijing, China

ARTICLE INFO

Article history:

Received 13 October 2015

Received in revised form

25 April 2016

Accepted 29 April 2016

Available online 6 June 2016

Keywords:

Burn-in

Degradation model

Gibbs sampling

Hierarchical Bayesian model

Reliability

ABSTRACT

Motivated by the two-phase degradation phenomena observed in light displays (e.g., plasma display panels (PDPs), organic light emitting diodes (OLEDs)), this study proposes a new degradation-based burn-in testing plan for display products exhibiting two-phase degradation patterns. The primary focus of the burn-in test in this study is to eliminate the initial rapid degradation phase, while the major purpose of traditional burn-in tests is to detect and eliminate early failures from weak units. A hierarchical Bayesian bi-exponential model is used to capture two-phase degradation patterns of the burn-in population. Mission reliability and total cost are introduced as planning criteria. The proposed burn-in approach accounts for unit-to-unit variability within the burn-in population, and uncertainty concerning the model parameters, mainly in the hierarchical Bayesian framework. Available pre-burn-in data is conveniently incorporated into the burn-in decision-making procedure. A practical example of PDP degradation data is used to illustrate the proposed methodology. The proposed method is compared to other approaches such as the maximum likelihood method or the change-point regression.

© 2016 Elsevier Ltd. All rights reserved.

1. Introduction

Burn-in is an important screening method to weed out weak or defective products before shipping to customers [1]. It is generally conducted by running products for a pre-determined amount of time under designed or accelerated stress conditions [2,3]. Conventional burn-in tests identify defective or weak products by inducing their failures over the testing periods (referred to as *failure-based* burn-in tests hereafter). Various aspects of failure-based burn-in tests, including test durations, stress types and levels, and residual-life distributions after burn-in, have been investigated by numerous researchers over the past four decades (e.g., [4–8]). Most research centers on how long and under what conditions the burn-in process should be conducted to maximize cost efficiency and field reliability. Comprehensive reviews of failure-based burn-in test design have been conducted by Kuo et al. [1] and Liu and Mazzuchi [9].

For highly reliable products, traditional failure-based burn-in tests may be ineffective because long burn-in duration may be required to observe failures [10]. Now, along with degradation data for performance measures related to product failures,

degradation-based burn-in tests are being considered as a promising alternative to failure-based burn-in tests [11]. Previous studies on degradation have focused on developing degradation models to estimate failure-time distributions [12–19], predicting remaining useful life distribution for a unit being monitored [20–23], and exploring preventive maintenance policies for continuous monitoring of degrading products [24–26]. Some recent studies considered degradation-based burn-in models and methods. Tseng and Tang [27] proposed a cost-optimal burn-in policy via a Wiener process degradation model. Under the assumption that there exists some proportion of weak products in the population, they proposed a total cost function consisting of burn-in operation cost, measurement cost, and misclassification cost. The burn-in decision variables they used were burn-in duration and the cutoff point. At the end of burn-in, if a unit's degradation level exceeded the cutoff point, it was classified as a weak unit. Tseng and Peng [28], Tseng et al. [11], and Tsai et al. [29] later explored this degradation-based burn-in approach to create several burn-in testing protocols. Tseng and Peng [28] introduced an integrated Wiener process to describe cumulative degradation, then derived an optimal burn-in policy based on the cumulative degradation model. Tseng et al. [11] proposed a burn-in procedure with multiple cutoff points. Tsai et al. [29] assumed that the underlying degradation pattern followed a gamma process instead of the Wiener process. Xiang et al. [30], Ye et al. [31], Peng et al. [32], and Feng et al. [33]

E-mail addresses: yuan@ohio.edu (T. Yuan), sjbae@hanyang.ac.kr (S.J. Bae), xzhu5@ucas.ac.cn (X. Zhu).

considered simultaneous optimization of burn-in and preventive maintenance with the decision variables corresponding to burn-in duration, cutoff point, and replacement interval. Ye et al. [10] planned burn-in tests considering two competing failure modes: soft (degradation-threshold) failure and catastrophic failure. Zhai et al. [34] considered measurement errors in degradation based burn-in. They used Wiener process to model the underlying degradation and considered Gaussian measurement errors in the observations.

All of the aforementioned studies on the degradation-based burn-in tests assumed that the burn-in population consists of weak and normal units, and that the main purpose of burn-in is to identify the weak ones based on the degradation data collected in the burn-in tests. The heterogeneity of the burn-in population is usually modeled by a mixture degradation model (e.g., the mixed Wiener process, the mixed gamma process) [11,27–31] or a random-effect degradation model [10,32,33]. However, motivated by the two-phase degradation phenomenon observed in light displays, this study considers a different type of burn-in planning problem for products exhibiting two-phase degradation patterns.

An industrial collaborator conducted a degradation test on six plasma display panels (PDPs) to assess their reliability at a constant stress level. The six individual PDP degradation paths, which were analyzed by Bae et al. [16], consist of relative luminosity measurements inspected regularly. As shown in Fig. 1, after a rapid decrease in brightness at the initial stage of the degradation testing, the decrease in paths slowed. Bae et al. [16] explained the degradation physics concerning this two-phase degradation phenomenon for PDPs. During the PDP manufacturing process, impurities remain inside the PDPs, and due to a temporary “poisoning effect” of the impurities, the light display will initially experience a rapid decrease in light intensity until the impurities are completely burned out, at which time the light degradation will continue at a slower, more stable rate [16]. PDP manufacturers execute a burn-in procedure (called “aging” in the industry) to burn off the impurities. The major purpose of this burn-in procedure is to eliminate the initial rapid degradation phase before shipping to customers. Infant mortality (i.e., early failures of weak products) is not a major concern in terms of luminosity degradation. Many other products such as organic light-emitting diodes (OLEDs) [35], lithium-ion batteries [36], and direct methanol fuel cells [37] have similar two-phase degradation patterns. Therefore, the proposed burn-in methods described in this study have

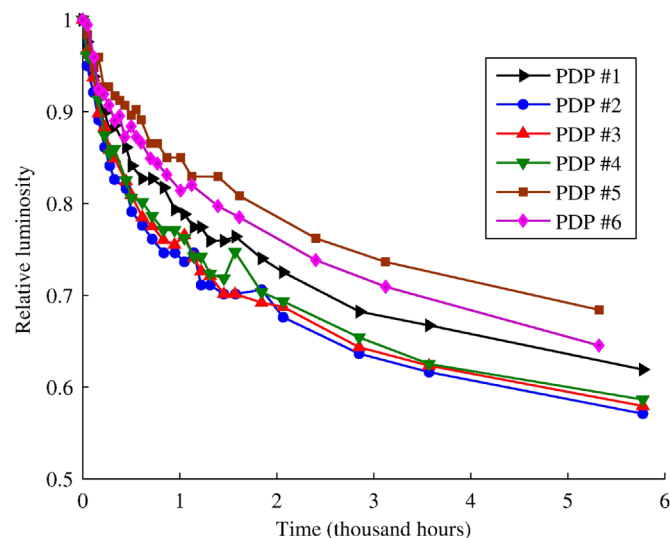


Fig. 1. Observed degradation paths of six PDPs: relative luminosity vs. measurement time.

potential application for those products as well.

This study used the Bayesian approach to plan degradation-based burn-in tests. Traditional maximum likelihood based burn-in planning methods usually assume that the model parameters are known before planning and conducting the burn-in test. However, in actual situations, uncertainties in the model parameters dominate the burn-in test environments [9]. In such cases, Bayesian methods are more appropriate and have been proven to be effective in planning failure-based burn-in tests [7,8]. This study adopts the Bayesian framework in degradation-based burn-in test planning methodology.

The remainder of this paper is organized as follows. The proposed methodology is presented in Section 2. Both reliability and cost criteria are considered, and the associated Bayesian computational methods are developed. The PDP example used by Bae et al. [16] is revisited to illustrate the proposed methodology in Section 3. Finally, this study is concluded and future research directions are outlined in Section 4.

2. Methodology

This section presents the proposed burn-in methodology using PDPs as an illustrative example. The actual degradation path of a unit is a monotonic decreasing function of the deterioration of a quality or performance characteristic over time. In degradation analysis, a “soft” failure is usually defined in terms of the amount of degradation to a critical threshold level. In display industry, when manufacturers ship the display products like PDPs and OLEDs to customers, they set initial display brightness to the level which is requested by the customers, and a display unit is considered to have failed when its luminosity falls below 50% of its initial value [16]. Therefore, the relative luminosity, instead of the luminosity, is selected as the performance characteristic.

2.1. Degradation modeling

A degradation model adequately describing the two-phase degradation path is essential for planning burn-in tests. Two different modeling approaches have been proposed in the literature. Bae and Kvam [38] developed a change-point regression model to describe the two-phase degradation patterns of PDPs. Bae et al. [16] employed a bi-exponential model for the PDP degradation paths. The bi-exponential model was also applied to describe the two-phase degradation of direct methanol fuel cells [37]. This study adopts the bi-exponential degradation model because it provides a better fit for the PDP degradation data than the change-point regression model [39].

The expected degradation path of a unit randomly selected from the burn-in population is described by the following non-linear function [16]

$$\eta(t; \gamma_1, \gamma_2, \varphi) = \varphi \exp(-\gamma_1 t) + (1 - \varphi) \exp(-\gamma_2 t), \quad (1)$$

where $\eta(\cdot)$ represents the expected degradation path of the relative luminosity, $\varphi \in (0, 1)$ denotes the initial proportion of impurities, and $\gamma_1 > 0$ and $\gamma_2 > 0$ represent the impurities' degradation rate and the inherent degradation rate of plasma phosphors, respectively. Because the impurities' degradation rate, γ_1 , is expected to be greater than the inherent degradation rate, γ_2 , we reparameterize the bi-exponential model (1) as

$$\eta(t; \theta) = \varphi \exp(-(\gamma + \Delta\gamma)t) + (1 - \varphi) \exp(-\gamma t), \quad (2)$$

where $\gamma > 0$ represents the inherent degradation rate of plasma phosphors, and $(\gamma + \Delta\gamma)$ denotes the impurities' degradation rate. Letting $\Delta\gamma > 0$ can yield the desired two-phase degradation

patterns. Herein $\theta = (\varphi, \gamma, \Delta\gamma)$. To account for unit-to-unit variability in the population, the degradation-path parameters θ are assumed to be random with a multivariate distribution $f_{\Theta}(\theta|\phi)$ and a parameter vector ϕ , i.e., $\theta \sim f_{\Theta}(\theta|\phi), \forall \theta \in \Theta$. Herein, Θ represents the parameter space for θ . Finally, prior knowledge concerning uncertainty in the parameter vector ϕ is expressed by a prior distribution denoted by $f_{\Phi}(\phi), \phi \in \Phi$, where Φ is the parameter space for ϕ . In summary, the degradation path Eq. (2), $\theta \sim f_{\Theta}(\theta|\phi)$, and $\phi \sim f_{\Phi}(\phi)$ form a three-stage hierarchical Bayesian model to describe the expected degradation of a random unit from the burn-in population.

In degradation analysis, a “soft” failure is usually defined in terms of the amount of degradation to a critical threshold level. For instance, in display industries, a critical quality measure is luminosity, and a display unit is considered to have failed when its luminosity falls below 50% of its initial value [16].

The mission reliability, $R(t_m)$, is the probability that a random unit released to operation can survive for a pre-specified mission time t_m . Conditioning on a given ϕ , the mission reliability without burn-in is defined as

$$R(t_m|\phi) = \Pr(T > t_m|\phi) = \int_{\Theta} \Pr(\eta(t_m; \theta) > \eta^*) f_{\Theta}(\theta|\phi) d\theta, \quad (3)$$

where T denotes the time-to-soft-failure, and η^* denotes the degradation threshold for the soft failure. For example, $\eta^* = 50\%$ for each PDP. In the Bayesian framework, all model parameters, e.g., ϕ , are random variables, and, hence, any functions of the model parameters, e.g., $R(t_m)$, are also random variables. The prior distribution for the mission reliability $R(t_m)$, denoted by $f_{R_m}(r)$ can, therefore, be derived from the prior distribution of ϕ , $f_{\Phi}(\phi)$, via transformation of random variables according to Eq. (3). The prior mean mission reliability $E[R(t_m)]$ is, then, defined as

$$E[R(t_m)] = \int_0^1 r f_{R_m}(r) dr = \int_{\Phi} \left(\int_{\Theta} \Pr(\eta(t_m; \theta) > \eta^*) f_{\Theta}(\theta|\phi) d\theta \right) f_{\Phi}(\phi) d\phi,$$

where $f_{R_m}(r)$ and $E(R_m)$ have no closed-form expressions, and Monte Carlo simulation methods can be used to estimate them. This study only considers the degradation-based soft failure mode and the catastrophic failure mode (or called the hard failure mode) is not included. If one needs to consider both failure modes, a competing-risk reliability model can be employed.

2.2. Reliability criterion

As shown in a previous study on PDP degradation [38], the initial rapid degradation phase caused by impurities significantly reduces the field reliability perceived by customers. Removing the rapid degradation phase through burn-in is essential to the improvement of field reliability and customer satisfaction. This section presents a reliability criterion based on the mission reliability used to plan the burn-in test.

Assume all units are subject to a degradation-based burn-in test at the designed operation conditions, and the burn-in duration is denoted by t_b . Upon completion of the burn-in degradation test, a unit is released to customers if its end-of-burn-in degradation level does not fall below a cutoff value denoted by η_b . We consider two scenarios of η_b . In the first scenario, η_b is fixed at 0%, which means that there is no end-of-burn-in inspection and all units are released to customers after burn-in. This scenario eliminates the rapid initial degradation phase. The burn-in duration t_b is the only decision variable in the burn-in planning problem. In the second scenario, the burn-in duration t_b and the cutoff point η_b are both decision variables. In this scenario, the purposes of the burn-in degradation test are to eliminate the rapid degradation phase and reject weak units.

Conditioning on a given ϕ , the mission reliability of a unit that

passed the degradation burn-in test is defined as

$$\begin{aligned} R(t_m|t_b, \eta_b, \phi) &= \Pr(T > t_m + t_b | T > t_b, \phi) \\ &= \int_{\Theta} \Pr\left(\frac{\eta(t_m + t_b; \theta)}{\eta(t_b; \theta)} > \eta^* | \eta(t_b; \theta) > \eta_b\right) f_{\Theta}(\theta|\phi) d\theta, \end{aligned}$$

where $T > t_b$ indicates that a unit is released to customers after burn-in because its end-of-burn-in degradation level does not fall below the cutoff value η_b , i.e., $\eta(t_b; \theta) > \eta_b$. The time-to-failure for a random unit released to field operation after burn-in is defined as the relative luminosity $\eta(t + t_b; \theta)/\eta(t_b; \theta)$ less than η^* because the initial luminosity perceived by the customers is the luminosity at the end of the burn-in test. The prior mean mission reliability after burn-in is, then, defined by

$$E[R(t_m|t_b, \eta_b)] = \int_{\Phi} \left[\int_{\Theta} \Pr\left(\frac{\eta(t_m + t_b; \theta)}{\eta(t_b; \theta)} > \eta^* | \eta(t_b; \theta) > \eta_b\right) f_{\Theta}(\theta|\phi) d\theta \right] f_{\Phi}(\phi) d\phi. \quad (4)$$

The reliability criterion $E[R(t_m|t_b, \eta_b)]$ defined in Eq. (4) does not have a closed-form expression, but can be evaluated using the following Monte Carlo simulation algorithm:

- (i) Simulate many ϕ vectors from $f_{\Phi}(\phi), \phi \in \Phi$;
- (ii) For each ϕ vector obtained in Step (i), simulate a θ vector from $f_{\Theta}(\theta|\phi), \theta \in \Theta$;
- (iii) For all θ vectors obtained in Step (ii), compute the ratio between the number of θ vectors satisfying both $\eta(t_m + t_b; \theta)/\eta(t_b; \theta) > \eta^*$ and $\eta(t_b; \theta) > \eta_b$ and the number of θ vectors satisfying only $\eta(t_b; \theta) > \eta_b$. This ratio provides an estimate of the $E[R(t_m|t_b, \eta_b)]$ criterion.

If the search space contains a finite number of candidate plans, it may be possible to enumerate all candidate plans, compute their $E[R(t_m|t_b, \eta_b)]$ values, and choose the desired plan. If it is infeasible to enumerate all candidate plans, the surface smoothing technique proposed by Muller and Parmigiani [40] could be used. In brief, this technique chooses a set of candidate plans spread over the search space, computes the planning criterion values for these selected plans, fits a smooth surface using the method of kernels, and finally searches for the desired plan on that smoothed surface.

2.3. Cost criterion

In this section, a cost criterion for planning the degradation-based burn-in tests is presented. We adopt and extend the general cost model discussed by Yuan and Kuo [8] and Perlstein et al. [7] for planning failure-based burn-in tests. Three types of costs are considered: the costs of the burn-in procedures, the costs associated with rejection of weak units after burn-in, and the costs of failures in field operation during the warranty period, t_w . Let C_{bs} , C_{bv} , C_{bf} , and C_{wf} denote the fixed burn-in cost per unit, the variable burn-in cost per unit per unit time, the burn-in rejection cost per unit, and the failure cost per unit during field operation. The expected cost per burn-in unit conditioning on a given ϕ can be expressed by

$$\begin{aligned} E(C|t_b, \eta_b, \phi) &= C_{bs} + C_{bv}t_b + C_{bf}\Pr(T < t_b|t_b, \eta_b, \phi) + C_{wf}\Pr(T > t_b \\ &\quad |t_b, \eta_b, \phi)\Pr(T < t_b + t_w|T > t_b, t_b, \eta_b, \phi) \\ &= C_{bs} + C_{bv}t_b + C_{bf}\Pr(T < t_b|t_b, \eta_b, \phi) \\ &\quad + C_{wf}\Pr(t_b < T < t_b + t_w|t_b, \eta_b, \phi), \end{aligned} \quad (5)$$

where $T < t_b$ denotes the event in which a unit is rejected at the end of burn-in because $\eta(t_b; \theta) < \eta_b$, $\Pr(T < t_b|t_b, \eta_b, \phi) = \int_{\Theta} \Pr(\eta(t_b; \theta) < \eta_b) f_{\Theta}(\theta|\phi) d\theta$, and $\Pr(t_b < T < t_b + t_w|t_b, \eta_b, \phi) = \int_{\Theta} \Pr(\eta(t_b; \theta) > \eta_b \cap \eta(t_b + t_w; \theta)/\eta(t_b; \theta) < \eta^*) f_{\Theta}(\theta|\phi) d\theta$. Note that the term $C_{bf}\Pr(T < t_b|t_b, \eta_b, \phi)$ in Eq. (5) is called the burn-in

rejection cost instead of the burn-in failure cost as in traditional failure-based burn-in tests. The degradation-based burn-in test rejects a unit if its end-of-burn-in degradation level is below the cutoff value η_b , which does not mean that the unit has failed during the burn-in test because η_b is expected to be higher than the failure threshold η^* due to the short burn-in duration. On the other hand, it is possible that a unit's degradation level at the end of the burn-in test is below the failure threshold η^* , and that unit will be rejected. Therefore, the cost of failed products during the burn-in test is included in the burn-in rejection cost.

Taking into account the prior uncertainty in ϕ , measured by the prior distribution $f_\phi(\phi)$, the prior expected cost is given by

$$E(C|t_b, \eta_b) = \int_{\Phi} E(C|t_b, \eta_b, \phi) f_\phi(\phi) d\phi = C_{bs} + C_{bv}t_b + C_{bf} \Pr(T < t_b | t_b, \eta_b) + C_{wf} \Pr(t_b < T < t_b + t_w | t_b, \eta_b),$$

where $\Pr(T < t_b | t_b, \eta_b) = \int_{\Phi} \Pr(T < t_b | t_b, \eta_b, \phi) f_\phi(\phi) d\phi$, and $\Pr(t_b < T < t_b + t_w | t_b, \eta_b) = \int_{\Phi} \Pr(t_b < T < t_b + t_w | t_b, \eta_b, \phi) f_\phi(\phi) d\phi$.

$\Pr(T < t_b | t_b, \eta_b)$ and $\Pr(t_b < T < t_b + t_w | t_b, \eta_b)$ need to be computed in order to evaluate the cost criterion $E(C|t_b, \eta_b)$ for a candidate plan (t_b, η_b) . The Monte Carlo simulation algorithm presented in Section 2.2 can be modified for this evaluation. In Step (iii), $\Pr(T < t_b | t_b, \eta_b)$ is estimated by the fraction of simulated θ vectors that satisfy $\eta(t_b; \theta) < \eta_b$, and $\Pr(t_b < T < t_b + t_w | t_b, \eta_b)$ is evaluated by the fraction of simulated θ vectors satisfying both $\eta(t_b; \theta) > \eta_b$ and $\eta(t_b + t_w; \theta) / \eta(t_b; \theta) < \eta^*$.

2.4. Incorporation of pre-burn-in data

A distinctive advantage of the Bayesian approach is that it updates prior knowledge with the addition of new data from pre-burn-in test data or from previous burn-in data.

Let $\mathbf{d} \equiv \{(y_{ij}, t_{ij}) : i = 1, 2, \dots, n; j = 1, 2, \dots, m_i\}$ denote the pre-burn-in data of n units. Herein, y_{ij} is the j th response on the i th unit measured at time t_{ij} , m_i is the number of measurements on the i th unit. A three-stage hierarchical Bayesian degradation model is formulated as follows.

The first-stage model describes the observed degradation data by

$$y_{ij} = \eta(t_{ij}; \theta_i) + \epsilon_{ij} = \varphi_i \exp(-\gamma_{1i} t_{ij}) + (1 - \varphi_i) \exp(-\gamma_{2i} t_{ij}) + \epsilon_{ij}, \quad i = 1, 2, \dots, n; \quad j = 1, 2, \dots, m_i, \quad (6)$$

where $\theta_i \equiv (\varphi_i, \gamma_{1i}, \gamma_{2i})$, for $i = 1, 2, \dots, n$, and ϵ_{ij} , which denotes the random measurement error of the i th unit at time t_{ij} , is assumed to be *iid* normal with mean zero and variance σ^2 and independent of θ_i 's. The second-stage model accounts for the unit-to-unit variability by assuming that all θ_i 's come from a common multivariate distribution, i.e., $\theta_i \sim f_\theta(\theta_i | \phi)$, $i = 1, 2, \dots, n$. Finally, the third-stage model completes the model specification by assigning independent prior distributions $f_\phi(\phi)$ and $f_\Sigma(\sigma^2)$, where Σ is the parameter space for σ^2 .

According to the Bayes' theorem, the joint posterior distribution of all model parameters is derived by

$$f(\theta_1, \theta_2, \dots, \theta_n, \sigma^2, \phi | \mathbf{d}) \propto \prod_{i=1}^n \prod_{j=1}^{m_i} (\sigma^2)^{-1/2} \exp\left\{-\frac{[y_{ij} - \eta(t_{ij}; \theta_i)]^2}{2\sigma^2}\right\} \times \prod_{i=1}^n f_\theta(\theta_i | \phi) \times f_\phi(\phi) \times f_\Sigma(\sigma^2).$$

Then the marginal posterior distribution of ϕ can be obtained by integrating out other model parameters, i.e.,

$$f_\phi(\phi | \mathbf{d}) = \int_{\Theta} \int_{\Theta} \dots \int_{\Theta} \int_{\Sigma} f(\theta_1, \theta_2, \dots, \theta_n, \sigma^2, \phi | \mathbf{d}) d\sigma^2 d\theta_1, d\theta_2, \dots, d\theta_n. \quad (7)$$

It is analytically intractable to compute the marginal posterior distribution $f_\phi(\phi | \mathbf{d})$ given by Eq. (7) because of the involvement of high-dimensional integration. Markov chain Monte Carlo (MCMC) simulation based algorithms, e.g., Gibbs sampling, can be employed instead to obtain a random sample from the marginal posterior distribution $f_\phi(\phi | \mathbf{d})$.

Each iteration of Gibbs sampling cycles through the unknown parameters, drawing a sample of one parameter conditional on the latest values of all the others. It is convenient to derive the conditional posterior distributions required by the Gibbs sampling, i.e., $f(\phi | \theta_1, \dots, \theta_n, \sigma^2, \mathbf{d})$, $f(\sigma^2 | \theta_1, \dots, \theta_n, \phi, \mathbf{d})$, and $f(\theta_i | \theta_1, \dots, \theta_{i-1}, \theta_{i+1}, \dots, \theta_n, \sigma^2, \phi, \mathbf{d})$, for $i = 1, 2, \dots, n$, and sample from these conditional posterior distributions using modern sampling techniques. When the number of iterations is large enough, the samples drawn on one parameter can be regarded as simulated observations from its marginal distribution. For example, the ϕ vectors drawn from the conditional posterior distribution $f(\phi | \theta_1, \dots, \theta_n, \sigma^2, \mathbf{d})$ can be regarded as a random sample from the marginal posterior distribution of ϕ , i.e., $f_\phi(\phi | \mathbf{d})$ defined by Eq. (7).

Replacing the prior distribution $f_\phi(\phi)$ in the reliability criterion (4) and the cost criterion (6) with the posterior distribution $f_\phi(\phi | \mathbf{d})$ yields the posterior mean mission reliability defined by

$$E[R(t_m | t_b, \eta_b, \mathbf{d})] = \int_{\Phi} \left[\int_{\Theta} \Pr\left(\frac{\eta(t_m + t_b; \theta)}{\eta(t_b; \theta)} > \eta^* \eta(t_b; \theta) > \eta_b\right) f_\theta(\theta | \phi) d\theta \right] f_\phi(\phi | \mathbf{d}) d\phi, \quad (8)$$

and the posterior expected cost

$$E(C|t_b, \eta_b, \mathbf{d}) = C_{bs} + C_{bv}t_b + C_{bf} \Pr(T < t_b | t_b, \eta_b, \mathbf{d}) + C_{wf} (\Pr(t_b < T < t_b + t_w | t_b, \eta_b, \mathbf{d})), \quad (9)$$

where $\Pr(T < t_b | t_b, \eta_b, \mathbf{d}) = \int_{\Phi} \left[\int_{\Theta} \Pr(\eta(t_b; \theta) < \eta_b) f_\theta(\theta | \phi) d\theta \right] f_\phi(\phi | \mathbf{d}) d\phi$, and $\Pr(t_b < T < t_b + t_w | t_b, \eta_b, \mathbf{d}) = \int_{\Phi} \left[\int_{\Theta} \Pr(\eta(t_b; \theta) > \eta_b \cap \eta(t_b + t_w; \theta) / \eta(t_b; \theta) < \eta^*) f_\theta(\theta | \phi) d\theta \right] f_\phi(\phi | \mathbf{d}) d\phi$.

Step (i) in the simulation algorithm presented in Section 2.2 needs to be modified by generating ϕ vectors from the posterior distribution $f_\phi(\phi | \mathbf{d})$, which are obtained using Gibbs sampling.

3. PDP example

In this section, the PDP example shown in Fig. 1 is used to illustrate the proposed burn-in methodology. Incorporating the available pre-burn-in test data of the six PDPs, we apply the two posterior criteria, $E[R(t_m | t_b, \eta_b, \mathbf{d})]$ and $E(C|t_b, \eta_b, \mathbf{d})$, defined in Eqs. (8) and (9), respectively, to plan the burn-in test.

In the second stage of the hierarchical Bayesian degradation model, the multivariate distribution $f_\theta(\theta | \phi)$ is assumed to be a truncated trivariate normal distribution

$$\theta \equiv (\varphi, \gamma, \Delta\gamma) \sim \mathcal{N}_3(\boldsymbol{\mu}, \boldsymbol{\Sigma}) \mathcal{I}_{(0 < \varphi < 1, \gamma > 0, \Delta\gamma > 0)},$$

where $\boldsymbol{\mu}$ and $\boldsymbol{\Sigma}$ are the mean vector and the covariance matrix, respectively, and $\mathcal{I}_{\{\cdot\}}$ is an indicator function.

The third stage of the model specifies prior distributions for $\phi \equiv (\boldsymbol{\mu}, \boldsymbol{\Sigma})$ and σ^2 . Prior distributions play a critical role in the Bayesian models. Conjugate priors, when available, simplify the posterior computation. If prior information is not available, non-informative priors are desired. In this example, we intend to use non-informative priors because of our lack of prior knowledge. The conjugate prior for σ^2 is the inverse-gamma ($IG(a_\sigma, b_\sigma)$)

distribution, where a_σ and b_σ are the shape and scale parameters, respectively. We assign σ^2 the $\mathcal{IG}(1, 0.0001)$ prior distribution, which is a popular non-informative prior used in the Bayesian literature [41]. The conditional conjugate prior for the mean vector and the covariance matrix of a non-truncated multivariate normal distribution is the independent normal-Wishart prior, i.e., a multivariate normal prior for the mean vector, and an inverse-Wishart ($\mathcal{IW}(\rho, \mathbf{S})$) prior for the covariance matrix. Herein, ρ is the degrees of freedom, and \mathbf{S} is a 3×3 symmetric positive-definite scale matrix. Therefore, we assign the mean vector $\boldsymbol{\mu}$ a trivariate normal prior $\mathcal{N}_3(\mathbf{0}_3, 10^6 \mathbf{I}_3)$, where $\mathbf{0}_3$ and \mathbf{I}_3 denote a zero vector of length three and a 3×3 identity matrix, respectively. Note that the large variance makes this distribution a non-informative prior for $\boldsymbol{\mu}$. Although using the inverse-Wishart prior distribution for the covariance matrix is computationally convenient, it is difficult to choose parameters for the inverse-Wishart distribution if a non-informative prior is needed for the covariance matrix. Thus, we adopt the scaled inverse-Wishart prior discussed by Barnard et al. [42]. The covariance matrix $\boldsymbol{\Sigma}$ is decomposed into variance and correlation components as $\boldsymbol{\Sigma} = \Delta \mathbf{Q} \Delta$, where the diagonal matrix $\Delta = \text{diag}(\delta_1, \delta_2, \delta_3)$ with $\delta_i > 0$ for $i = 1, 2, 3$, and \mathbf{Q} is a 3×3 symmetric positive-definite matrix. Then we assume a non-informative $\mathcal{IW}(4, \mathbf{I}_3)$ prior for the \mathbf{Q} matrix (i.e., the correlation components of the $\boldsymbol{\Sigma}$ matrix), and gamma $\mathcal{G}(a_\delta, b_\delta)$ priors for $\delta_k, k = 1, 2, 3$. The scale parameter a_δ and the shape parameter b_δ are set to 1 and 0.0001, respectively, resulting in non-informative priors for δ_k 's (i.e., the standard deviation components of the $\boldsymbol{\Sigma}$ matrix).

The posterior simulation is implemented using WinBUGS, a free software package for the Bayesian analysis of complex statistical models using MCMC methods [43]. Convergence of the simulation is monitored and verified. A random sample of 50,000 $\boldsymbol{\phi}$ vectors is drawn from the marginal posterior distribution $f_{\boldsymbol{\phi}}(\boldsymbol{\phi}|\mathbf{d})$ defined in Eq. (7).

Table 1 summarizes the posterior estimates of the first-stage parameters, $\boldsymbol{\theta}_i \equiv (\phi_i, \gamma_i, \Delta\gamma_i)$, in the hierarchical Bayesian bi-exponential degradation model applied to the PDP example. The posterior medians for $\boldsymbol{\mu}$ and $\boldsymbol{\Sigma}$ in the second stage of the model are

$$\begin{bmatrix} 0.1888 \\ 0.05402 \\ 2.718 \end{bmatrix} \quad \text{and} \quad \begin{bmatrix} 3.719 \times 10^{-3} & 4.278 \times 10^{-6} & 4.231 \times 10^{-3} \\ 4.278 \times 10^{-6} & 3.749 \times 10^{-6} & 4.220 \times 10^{-5} \\ 4.231 \times 10^{-3} & 4.220 \times 10^{-5} & 9.269 \times 10^{-2} \end{bmatrix}$$

respectively. Bae et al. [39] compared the performance from the bi-exponential degradation model to those from the change-point degradation model and a simple log-linear model applied to the PDP example, and observed that the bi-exponential model provided a better fit than the other models. The change-point degradation model will be discussed in Section 3.3. As an example, Fig. 2 shows the posterior mean degradation paths predicted by the three models for PDP #1. As shown in this figure, one short-coming with the change-point degradation model is that it produces an abrupt change in the mean degradation path at the change point.

3.1. Planning burn-in without inspection

First, we assume that the cutoff value η_b is fixed at zero. This means that there is no end-of-burn-in inspection, and all units are released to customers after burn-in. The burn-in duration, t_b , is the only decision variable. We assume the search space for t_b is 0 to 1000 h with an increment of one hour, and enumerate all candidate t_b values in the search space. Fig. 3 plots the posterior mean mission reliability $E[R(t_m|t_b, \eta_b, \mathbf{d})]$ against the burn-in duration t_b , assuming the mission duration $t_m = 10,000$ h. Without burn-in, the posterior mean mission reliability is only 25.2%. $E[R(t_m|t_b, \eta_b, \mathbf{d})]$ initially increases rapidly when t_b increases, and

Table 1
Posterior inference of the first-stage parameters, $\boldsymbol{\theta}_i$, in the hierarchical Bayesian bi-exponential model applied to the PDP example.

PDP, i	ϕ_i	γ_i	$\Delta\gamma_i$
	median (95% interval)	median (95% interval)	median (95% interval)
#1	0.1812 (0.1700, 0.1945)	0.05378 (0.04836, 0.05853)	2.682 (2.268, 3.100)
#2	0.2370 (0.2249, 0.2488)	0.05441 (0.04919, 0.06014)	3.032 (2.660, 3.523)
#3	0.2308 (0.2191, 0.2439)	0.05416 (0.04884, 0.05944)	2.689 (2.340, 3.040)
#4	0.2175 (0.2060, 0.2293)	0.05446 (0.04963, 0.05991)	2.770 (2.432, 3.152)
#5	0.1176 (0.1045, 0.1405)	0.05317 (0.04503, 0.05823)	2.500 (1.810, 3.066)
#6	0.1453 (0.1319, 0.1617)	0.05427 (0.04876, 0.06001)	2.609 (2.087, 3.113)

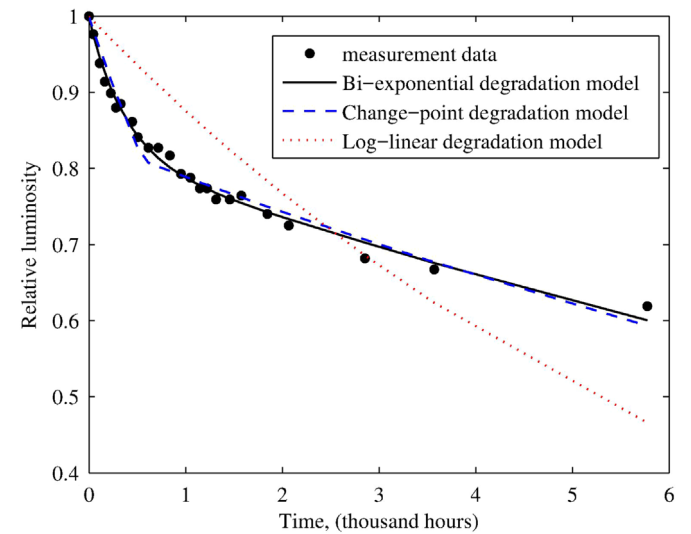


Fig. 2. Posterior mean degradation paths for PDP #1 predicted by the bi-exponential model, change-point degradation model, and log-linear model.

tends to saturate when t_b is above 600 h. Bae et al. [39] performed a Bayesian change-point regression analysis on the PDP data and found a posterior median of about 600 h for the transition time (i.e., the change point) between the initial rapid degradation phase and the later slower degradation phase. Therefore, when the burn-in time is around 600 h, we expect the initial rapid degradation phase to be completely eliminated. When a requirement for mean mission reliability is specified, we are able to find the minimum burn-in duration to achieve that requirement. For example, when a mean mission reliability of 90% is required, the minimum burn-in duration is 370 h.

Next, we plan the burn-in test according to the posterior expected cost criterion $E(C|t_b, \eta_b, \mathbf{d})$ defined in Eq. (9). For illustration purpose, we assume $C_{bs} = 10$, two different values for C_{bv} (i.e., 0.1 and 0.18), two different values for C_{wf} (i.e., 200 and 300), and $t_w = t_m = 10,000$ h. Only one value is assumed for C_{bs} because it does not affect the optimal burn-in duration. Since burn-in failures are not considered, $C_{bf} = 0$. Fig. 4 shows the posterior expected cost as a function of the burn-in duration for the four combinations of C_{bv} and C_{wf} values, and Table 2 summarizes the optimal burn-in durations. This cost-optimal burn-in plan represents a trade-off between the burn-in cost and the warranty cost, and is affected by the cost coefficients. As shown in Table 2, the cost-optimal burn-in duration, t_b^* , depends on the relative relationship between C_{bv} and

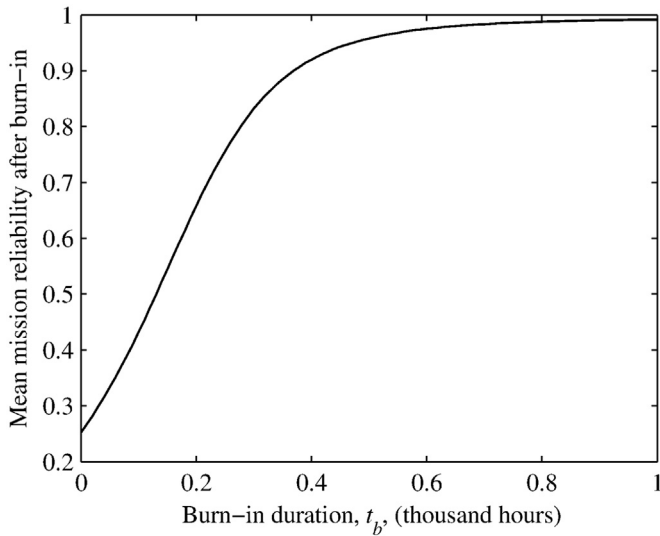


Fig. 3. The posterior mean mission reliability $E[R(t_m|t_b, \eta_b, \mathbf{d})]$ vs. the burn-in duration t_b when the cutoff value $\eta_b = 0$.

C_{wf} . As the ratio C_{bv}/C_{wf} increases, the burn-in costs increase, which leads to a reduction in the optimal burn-in duration. In addition, as the burn-in duration increases, the field failure probability after burn-in, $\Pr(t_b^* < T < t_b^* + t_w|t_b^*, \eta_b, \mathbf{d})$ decreases, which is consistent with the results presented in Fig. 3.

3.2. Planning burn-in with inspection

Now we consider the case with end-of-burn-in inspection. A unit is rejected if its end-of-burn-in degradation level falls below the cutoff value η_b . Fig. 5 shows the posterior mean mission reliability vs. the burn-in duration for different η_b values. It can be seen from this figure that for the same burn-in duration, increasing the cutoff value η_b improves the mission reliability after burn-in. When a mean mission reliability of 90% is desired, the minimum burn-in durations are listed in Table 3 for some different η_b values. As η_b increases, the minimum burn-in duration to achieve the desired mission reliability reduces. However, this reduction of burn-in duration is achieved by rejecting more units after burn-in, as shown in the $\Pr(T < t_b|t_b, \eta_b, \mathbf{d})$ column of Table 3. For example, when $\eta_b = 0.95$, after the 120-h burn-in duration, 66% of the burn-

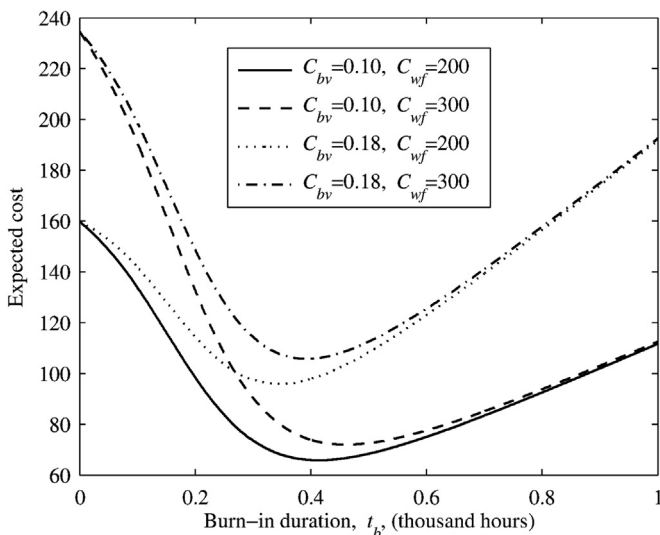


Fig. 4. The posterior expected cost $E[Cl(t_b, \eta_b, \mathbf{d})]$ vs. the burn-in duration t_b when the cutoff value $\eta_b = 0$ for different cost coefficients.

Table 2

Cost-optimal burn-in duration t_b^* for different cost coefficients, when $\eta_b = 0$.

C_{bv}	C_{wf}	C_{bv}/C_{wf}	t_b^* (h)	$\Pr(t_b^* < T < t_b^* + t_w t_b^*, \eta_b, \mathbf{d})$
0.10	300	0.0003	460	0.053
0.10	200	0.0005	410	0.074
0.18	300	0.0006	390	0.085
0.18	200	0.0009	343	0.121

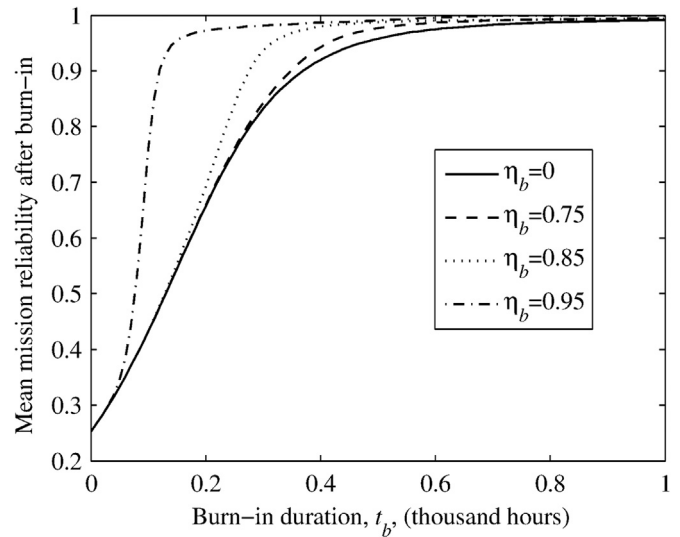


Fig. 5. The posterior mean mission reliability $E[R(t_m|t_b, \eta_b, \mathbf{d})]$ vs. the burn-in duration t_b for different η_b values.

in units would be rejected because their end-of-burn-in degradation levels are less than η_b . This may incur unnecessarily high burn-in rejection cost.

Next, the cost-optimal burn-in duration and cutoff value are obtained by minimizing the posterior expected cost criterion $E[Cl(t_b, \eta_b, \mathbf{d})]$ defined in Eq. (9). We assume that the candidate values for η_b are from 50% to 99% with an increment of 1%. Two different values, i.e., 100 and 150, are assumed for the burn-in failure cost C_{bf} . As an example, Fig. 6 shows the contour plot of the posterior expected cost when $C_{bs} = 10$, $C_{bv} = 0.1$, $C_{bf} = 100$, and $C_{wf} = 200$. Table 4 summarizes the cost-optimal burn-in plans (t_b^*, η_b^*) for the eight combinations of C_{bv} , C_{bf} , and C_{wf} values. We have the following observations. First, t_b^* and η_b^* are negatively correlated, that is, a longer burn-in duration tends to be accompanied with a lower cutoff value. This is due to the fact that the expected degradation path is assumed to be a monotonic decreasing function. Second, $\Pr(T < t_b^*|t_b^*, \eta_b^*, \mathbf{d})$, which is the probability that a unit is rejected after burn-in, and $\Pr(t_b^* < T < t_b^* + t_w|t_b^*, \eta_b^*, \mathbf{d})$, which is the probability that a unit released to customers after burn-in fails within the warranty period, are negatively correlated. These two probabilities directly impact the burn-in rejection cost and the field failure cost, respectively, and the optimal burn-in plans need to compromise

Table 3

Minimum burn-in duration to achieve the desired mission reliability for different cutoff values.

η_b	Minimum burn-in duration, t_b (h)	$\Pr(T < t_b t_b, \eta_b, \mathbf{d})$
0.00	370	–
0.75	350	0.024
0.85	280	0.187
0.95	120	0.660

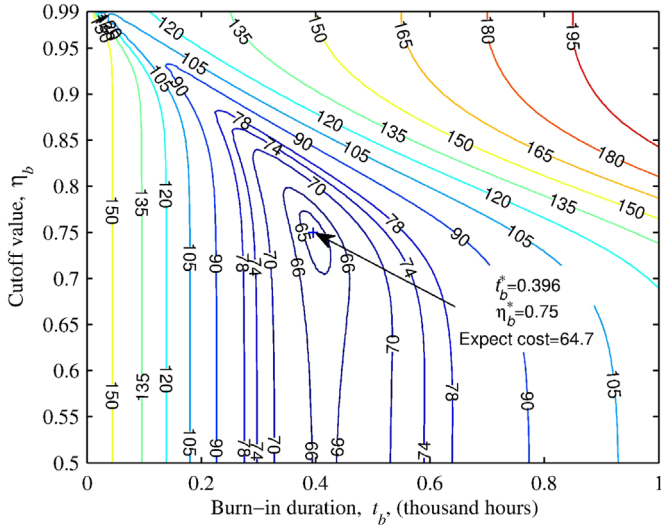


Fig. 6. Contour plot for the posterior expected cost $E(C|t_b, \eta_b, \mathbf{d})$ vs. the burn-in duration t_b and the cutoff value η_b , when $C_{bs} = 10$, $C_{bv} = 0.1$, $C_{bf} = 100$, and $C_{wf} = 200$.

Table 4
Cost-optimal burn-in plans (t_b^*, η_b^*) for different cost coefficients.

C_{bf}	C_{bv}	C_{wf}	t_b^* (h)	η_b^*	$\Pr(T < t_b^* t_b^*, \eta_b^*, \mathbf{d})$	$\Pr(t_b^* < T < t_b^* + t_w t_b^*, \eta_b^*, \mathbf{d})$
100	0.10	200	396	0.75	0.036	0.057
100	0.18	200	319	0.81	0.085	0.085
100	0.10	300	425	0.75	0.045	0.042
100	0.18	300	330	0.82	0.127	0.059
150	0.10	200	411	0.68	0.009	0.066
150	0.18	200	334	0.76	0.026	0.107
150	0.10	300	452	0.70	0.018	0.044
150	0.18	300	369	0.77	0.047	0.067

these cost terms. Third, for a given C_{bf} value, the optimal burn-in duration t_b^* again depends on the relative relationship between C_{bv} and C_{wf} . Finally, for the same set of C_{bv} and C_{wf} values, a higher C_{bf} value causes the optimal burn-in plan to lower the burn-in rejection probability $\Pr(T < t_b^* | t_b^*, \eta_b^*, \mathbf{d})$. To lower this burn-in rejection probability, the optimal cutoff value is reduced, and the optimal burn-in duration is increased because the burn-in duration and the cutoff value are negatively correlated.

3.3. Comparison between the bi-exponential degradation model and change-point degradation model

For the purpose of comparison, the burn-in test is planned based on the change-point degradation model developed in [39]. The test procedure is summarized by the following three-stage hierarchical Bayesian model:

- (i) $\ln y_{ij} = g(t_{ij}; \theta_i^c) + \epsilon_{ij}^c = \begin{cases} \alpha_i t_{ij} - \beta_i t_{ij} + \epsilon_{ij}^c, & 0 \leq t_{ij} < \lambda_i, \\ \alpha_i t_{ij} - \beta_i \lambda_i + \epsilon_{ij}^c, & t_{ij} \geq \lambda_i, \end{cases}$
where $\theta_i^c \equiv (\alpha_i, \beta_i, \lambda_i)$ and $\epsilon_{ij}^c \sim \mathcal{N}(0, (\sigma^c)^2)$, for $i = 1, 2, \dots, n$ and $j = 1, 2, \dots, m_i$;
- (ii) $\theta_i^c \equiv (\alpha_i, \beta_i, \lambda_i) \sim \mathcal{N}_3(\boldsymbol{\mu}^c, \boldsymbol{\Sigma}^c) \mathcal{I}_{\{\alpha_i < 0, \beta_i > 0, 0 < \lambda_i < 5\}}$, for $i = 1, 2, \dots, n$;
- (iii) $(\sigma^c)^2 \sim \mathcal{IG}(1, 0.0001)$;
 $\boldsymbol{\mu}^c \sim \mathcal{N}_3(\mathbf{0}_3, 10^6 \mathbf{I}_3)$;
 $\boldsymbol{\Sigma}^c = \boldsymbol{\Delta}^c \mathbf{Q}^c \boldsymbol{\Delta}^c$, where $\boldsymbol{\Delta}^c = \text{diag}(\delta_1^c, \delta_2^c, \delta_3^c)$,
 $\mathbf{Q}^c \sim \mathcal{IW}(4, \mathbf{I}_4)$, $\delta_k^c \sim \mathcal{G}(1, 0.0001)$, for $k = 1, 2, 3$.

Herein and hereafter, the superscript “c” is added to the parameters in the change-point degradation model in order to distinguish them from the parameters used in the bi-exponential degradation model. In the change-point degradation model, the performance measure is the logarithm of the relative luminosity, $\ln y$. The actual degradation path of $\ln y$ is modeled by two linear lines connected at the change point λ . α is the slope of the line after the change point, and $(\alpha - \beta)$ is the slope of the line before the change point. See [39] for details on the posterior computation and results of the change-point degradation model applied to the PDP example.

To apply the change-point degradation model to plan the burn-in tests, the posterior mean mission reliability given by Eq. (8) is modified as

$$E[R(t_m | t_b, \eta_b, \mathbf{d})] = \int_{\Phi^c} \left[\int_{\Theta^c} \Pr(g(t_m + t_b; \theta^c) - g(t_b; \theta^c) > \ln \eta_b^* | g(t_b; \theta^c) > \ln \eta_b) f_{\Theta^c}(\theta^c | \Phi^c) d\theta^c \right] f_{\Phi^c}(\Phi^c | \mathbf{d}) d\Phi^c, \quad (10)$$

and the posterior expected cost remains the form of (9). However, $\Pr(T < t_b | t_b, \eta_b, \mathbf{d})$ and $\Pr(t_b < T < t_b + t_w t_b, \eta_b, \mathbf{d})$ are evaluated by

$$\Pr(T < t_b | t_b, \eta_b, \mathbf{d}) = \int_{\Phi^c} \left[\int_{\Theta^c} \Pr(g(t_b; \theta^c) < \ln \eta_b) f_{\Theta^c}(\theta^c | \Phi^c) d\theta^c \right] f_{\Phi^c}(\Phi^c | \mathbf{d}) d\Phi^c,$$

and

$$\Pr(t_b < T < t_b + t_w t_b, \eta_b, \mathbf{d}) = \int_{\Phi^c} \left[\int_{\Theta^c} \Pr(g(t_b; \theta^c) > \ln \eta_b \cap (g(t_b + t_w; \theta^c) - g(t_b; \theta^c)) < \ln \eta_b^*) f_{\Theta^c}(\theta^c | \Phi^c) d\theta^c \right] f_{\Phi^c}(\Phi^c | \mathbf{d}) d\Phi^c,$$

respectively, for the change-point degradation model.

Tables 5, 6, and 7 compare, respectively, the minimum burn-in durations to achieve a 90% mission reliability, the cost-optimal burn-in durations t_b^* when $\eta_b = 0$, and the cost-optimal burn-in plans (t_b^*, η_b^*) between the hierarchical Bayesian bi-exponential and change-point degradation models. It can be observed from these results that the burn-in test plans are sensitive to the degradation models used. The change-point degradation model tends to choose longer burn-in durations than the bi-exponential degradation model, because it tends to predict a longer duration of the rapid degradation phase due to the sharp transition between the two phases at the change point (see Fig. 2).

3.4. Comparison between the Bayesian method and the maximum likelihood method

This section compares the burn-in test plans produced by the Bayesian method to the maximum likelihood method using the bi-exponential degradation model. The observed degradation data are modeled by the bi-exponential degradation model given by Eq. (6), and the random degradation-path coefficient vectors, θ_i , are assumed to form a random sample from the multivariate normal distribution with a mean vector $\boldsymbol{\mu}$ and a covariance matrix $\boldsymbol{\Sigma}$. The maximum likelihood estimates of the model parameters $\boldsymbol{\mu}$, $\boldsymbol{\Sigma}$, and σ^2 can be obtained by maximizing the following likelihood function

Table 5
Comparison of the minimum burn-in durations to achieve the 90% mission reliability among three approaches.

η_b	Minimum burn-in duration, t_b , (h)		
	Bi-exponential model Bayesian	Change-point model Bayesian	Bi-exponential model Maximum likelihood
0.00	370	445	302
0.75	350	428	301
0.85	280	370	258
0.95	120	197	104

Table 6
Comparison of the cost-optimal burn-in durations t_b^* when $\eta_b = 0$ among three approaches.

C_{bv}	C_{wf}	t_b^* (h)		
		Bi-exponential model Bayesian	Change-point model Bayesian	Bi-exponential model Maximum likelihood
0.10	300	460	520	408
0.10	200	410	519	379
0.18	300	390	495	364
0.18	200	343	469	336

Table 7
Comparison of the cost-optimal burn-in plans (t_b^*, η_b^*) among three approaches.

C_{bf}	C_{bv}	C_{wf}	Bi-exponential Bayesian		Change-point Bayesian		Bi-exponential Maximum likelihood	
			t_b^* (h)	η_b^*	t_b^* (h)	η_b^*	t_b^* (h)	η_b^*
100	0.10	200	396	0.75	504	0.50	368	0.78
100	0.18	200	319	0.81	470	0.56	289	0.84
100	0.10	300	425	0.75	531	0.50	379	0.79
100	0.18	300	330	0.82	504	0.52	301	0.84
150	0.10	200	411	0.68	504	0.34	385	0.75
150	0.18	200	334	0.76	470	0.56	320	0.80
150	0.10	300	452	0.70	535	0.38	407	0.75
150	0.18	300	369	0.77	504	0.50	357	0.79

$$L(\boldsymbol{\mu}, \boldsymbol{\Sigma}, \sigma^2 | \mathbf{d}) = \prod_{i=1}^n \int_{\theta_1} \dots \int_{\theta_n} \left[\prod_{j=1}^{m_i} \frac{1}{\sqrt{2\pi\sigma^2}} \exp\left(-\frac{(y_{ij} - \eta(t_{ij}; \boldsymbol{\theta}_i))^2}{2\sigma^2}\right) \right] \times (2\pi)^{-3/2} |\boldsymbol{\Sigma}|^{-1/2} \exp\left(-\frac{1}{2}(\boldsymbol{\theta}_i - \boldsymbol{\mu})^T \boldsymbol{\Sigma}^{-1}(\boldsymbol{\theta}_i - \boldsymbol{\mu})\right) d\theta_n, \dots, d\theta_1.$$

The two-stage algorithm developed by Lu and Meeker [44] is adopted to obtain the maximum likelihood estimates $\hat{\boldsymbol{\mu}}, \hat{\boldsymbol{\Sigma}},$ and $\hat{\sigma}^2$. The mission reliability criterion is defined by

$$R(t_m | t_b, \eta_b; \hat{\boldsymbol{\mu}}, \hat{\boldsymbol{\Sigma}}) = \int_{\boldsymbol{\theta}} \Pr\left(\frac{\eta(t_m + t_b; \boldsymbol{\theta})}{\eta(t_b; \boldsymbol{\theta})} > \eta^* | \eta(t_b; \boldsymbol{\theta}) > \eta_b\right) f_{\boldsymbol{\theta}}(\boldsymbol{\theta} | \hat{\boldsymbol{\mu}}, \hat{\boldsymbol{\Sigma}}) d\boldsymbol{\theta},$$

where $f_{\boldsymbol{\theta}}(\boldsymbol{\theta} | \hat{\boldsymbol{\mu}}, \hat{\boldsymbol{\Sigma}})$ denotes the probability density function of the multivariate normal distribution with a mean vector $\hat{\boldsymbol{\mu}}$ and a covariance matrix $\hat{\boldsymbol{\Sigma}}$. Monte Carlo simulation can be used to evaluate $R(t_m | t_b, \eta_b; \hat{\boldsymbol{\mu}}, \hat{\boldsymbol{\Sigma}})$ by simulating many $\boldsymbol{\theta}$ vectors from $f_{\boldsymbol{\theta}}(\boldsymbol{\theta} | \hat{\boldsymbol{\mu}}, \hat{\boldsymbol{\Sigma}})$ and computing the ratio between the fraction of $\boldsymbol{\theta}$ vectors satisfying both $\eta(t_m + t_b; \boldsymbol{\theta})/\eta(t_b; \boldsymbol{\theta}) > \eta^*$ and $\eta(t_b; \boldsymbol{\theta}) > \eta_b$ and the fraction of $\boldsymbol{\theta}$ vectors satisfying only $\eta(t_b; \boldsymbol{\theta}) > \eta_b$.

The expected cost per burn-in unit is

$$E(C | t_b, \eta_b; \hat{\boldsymbol{\mu}}, \hat{\boldsymbol{\Sigma}}) = C_{bs} + C_{bv}t_b + C_{bf}\Pr(T < t_b | t_b, \eta_b; \hat{\boldsymbol{\mu}}, \hat{\boldsymbol{\Sigma}}) + C_{wf}(\Pr(t_b < T < t_b + t_w | t_b, \eta_b; \hat{\boldsymbol{\mu}}, \hat{\boldsymbol{\Sigma}})),$$

where $\Pr(T < t_b | t_b, \eta_b; \hat{\boldsymbol{\mu}}, \hat{\boldsymbol{\Sigma}}) = \int_{\boldsymbol{\theta}} \Pr(\eta(t_b; \boldsymbol{\theta}) < \eta_b) f_{\boldsymbol{\theta}}(\boldsymbol{\theta} | \hat{\boldsymbol{\mu}}, \hat{\boldsymbol{\Sigma}}) d\boldsymbol{\theta}$, and $\Pr(t_b < T < t_b + t_w | t_b, \eta_b; \hat{\boldsymbol{\mu}}, \hat{\boldsymbol{\Sigma}}) = \int_{\boldsymbol{\theta}} \Pr(\eta(t_b; \boldsymbol{\theta}) > \eta_b \cap \eta(t_b + t_w; \boldsymbol{\theta}) / \eta(t_b; \boldsymbol{\theta}) < \eta^*) f_{\boldsymbol{\theta}}(\boldsymbol{\theta} | \hat{\boldsymbol{\mu}}, \hat{\boldsymbol{\Sigma}}) d\boldsymbol{\theta}$. Again, Monte Carlo simulation can be adopted to evaluate these two probabilities.

Tables 5–7 also compare the burn-in plans between the Bayesian and maximum likelihood approaches using the bi-exponential degradation model. Although the two approaches produce comparable and consistent results, the discrepancy in results from these two methods is mainly due to their different assumptions on $\boldsymbol{\mu}$ and $\boldsymbol{\Sigma}$. The maximum likelihood method assumes that $\boldsymbol{\mu}$ and $\boldsymbol{\Sigma}$ are fixed quantities, and uses the point estimates $\hat{\boldsymbol{\mu}}$ and $\hat{\boldsymbol{\Sigma}}$ obtained from the pre-burn-in data to plan the burn-in tests. The maximum likelihood method, therefore, does not incorporate the uncertainty in $\boldsymbol{\mu}$ and $\boldsymbol{\Sigma}$ when planning the tests. On the other hand, the Bayesian method assumes that $\boldsymbol{\mu}$ and $\boldsymbol{\Sigma}$ are random variables, quantifying the uncertainty in $\boldsymbol{\mu}$ and $\boldsymbol{\Sigma}$ by their joint posterior distribution, $f_{\boldsymbol{\phi}}(\boldsymbol{\phi} | \mathbf{d})$, where $\boldsymbol{\phi} = (\boldsymbol{\mu}, \boldsymbol{\Sigma})$.

4. Conclusion

Some products, e.g., PDPs, OLEDs, lithium-ion batteries, and direct methanol fuel cells, were found to exhibit two-phase degradation patterns, i.e., an initial rapid degradation phase followed by a slower and more stable degradation phase. To ensure high field reliability, it is essential that the manufacturers execute an adequate degradation-based burn-in procedure before shipping. This study proposed a methodology for planning such burn-in tests. Both reliability and cost criteria were developed, and the associated Bayesian computational methods were designed. Available pre-burn-in degradation data can be incorporated in the burn-in decision-making process via the Bayesian prior-to-posterior updating mechanism. A practical exam based on the PDP degradation was used to illustrate the application of the proposed methodology.

This study assumes that the burn-in test is conducted at the designed stress conditions. In order to reduce the burn-in duration, the burn-in test can be performed at accelerated stress conditions. Planning burn-in tests based on accelerated degradation models and test data will be studied in the future. This study is based on the bi-exponential degradation-path model, and burn-in planning using other degradation-path or stochastic process models will be explored. Moreover, burn-in optimization considering both degradation-based soft failure mode and catastrophic hard failure mode deserves further studies.

Acknowledgment

This research work was partially supported by the National Science Foundation of China under grant NSFC# 71571178. The work of S. J. Bae was supported by Basic Science Research Program through the National Research Foundation of Korea funded by the Ministry of Education (No. 201500000002571), and Leading Core Technology Program sponsored by Defense Acquisition Program Administration and Agency for Defense Development under the project title ‘‘High-Performance PMD Technology for Guided Missiles’’.

References

[1] Kuo W, Chien WTK, Kim T. Reliability, yield, and stress burn-in. Boston, MA:

- Wiley; 1998.
- [2] Kuo W. Reliability enhancement through optimal burn-in. *IEEE Trans Reliab* 1984;33:145–56.
 - [3] Elsayed EA. Overview of reliability testing. *IEEE Trans Reliab* 2012;61:282–91.
 - [4] Cha JH, Finkelstein M. Stochastically ordered subpopulations and optimal burn-in procedure. *IEEE Trans Reliab* 2010;59:635–43.
 - [5] Shafiee M, Finkelstein M, Zuo MJ. Optimal burn-in and preventive maintenance warranty strategies with time-dependent maintenance costs. *IIE Trans* 2013;45:1033–2014.
 - [6] Ye Z-S, Tang LC, Xie M. Bi-objective burn-in modeling and optimization. *Ann Oper Res* 2014;212:201–14.
 - [7] Perlstein D, Jarvis WH, Mazzuchi TA. Bayesian calculation of cost optimal burn-in test durations for mixed exponential populations. *Reliab Eng Syst Saf* 2001;72:265–73.
 - [8] Yuan T, Kuo Y. Bayesian analysis of hazard rate, change point, and cost-optimal burn-in time for electronic devices. *IEEE Trans Reliab* 2010;59:132–8.
 - [9] Liu X, Mazzuchi TA. The optimal burn-in: state of the art and new advances for cost function formulation. In: Pham H, editor. *Recent advances in reliability and quality in design*, Springer, London, UK, p. 137–82.
 - [10] Ye Z-S, Xie M, Tang L-C, Shen Y. Degradation-based burn-in planning under competing risks. *Technometrics* 2012;54:159–68.
 - [11] Tseng S-T, Tang J, Ku I-H. Determination of burn-in parameters and residual life for highly reliable products. *Nav Res Logist* 2003;50:1–14.
 - [12] Lu CJ, Meeker WQ, Escobar LA. A comparison of degradation and failure-time analysis methods for estimating a time-to-failure distribution. *Stat Sin* 1996;6:531–46.
 - [13] Meeker WQ, Escobar LA, Lu CJ. Accelerated degradation tests: modeling and analysis. *Technometrics* 1998;40:89–99.
 - [14] Nikulin MS, Limnios N, Balakrishnan N, Kahle W, Huber-Carol C. *Advances in degradation modeling*. Boston, MA: Birkhauser; 2010.
 - [15] Bae SJ, Kvam PH. A nonlinear random-coefficients model for degradation testing. *Technometrics* 2004;46:460–9.
 - [16] Bae SJ, Kim SJ, Kim MS, Lee BJ, Kang CW. Degradation analysis of nano-contamination in plasma display panels. *IEEE Trans Reliab* 2008;57:222–9.
 - [17] Robinson M, Crowder MJ. Bayesian methods for a growth-curve degradation model with repeated measures. *Lifetime Data Anal* 2000;6:357–74.
 - [18] Ye Z-S, Wang Y, Tsui KL, Pecht M. Degradation data analysis using Wiener processes with measurement errors. *IEEE Trans Reliab* 2013;62:772–80.
 - [19] Ye Z-S, Chen N, Shen Y. A new class of Wiener process models for degradation analysis. *Reliab Eng Syst Saf* 2015;139:58–67.
 - [20] Gebraeel NZ, Lawley MA, Li R, Ryan JK. Residual-life distributions from component degradation signals: a Bayesian approach. *IIE Trans* 2005;37:543–57.
 - [21] Chen N, Tsui KL. Condition monitoring and remaining useful life prediction using degradation signals: revisited. *IIE Trans* 2013;45:939–52.
 - [22] Gebraeel NZ, Pan J. Prognostic degradation models for computing and updating residual life distribution in a time-varying environment. *IEEE Trans Reliab* 2008;57:539–50.
 - [23] Wang X, Balakrishnan N, Guo B. Residual life estimation based on a generalized Wiener degradation process. *Reliab Eng Syst Saf* 2014;124:13–23.
 - [24] Caballe NC, Castro IT, Perez CJ, Lanza-Gutierrez JM. A condition-based maintenance of a dependent degradation-threshold-shock model in a system with multiple degradation processes. *Reliab Eng Syst Saf* 2015;134:98–109.
 - [25] Hong HP, Zhou W, Zhang S, Ye W. Optimal condition-based maintenance decisions for systems with dependent stochastic degradation of components. *Reliab Eng Syst Saf* 2014;121:276–88.
 - [26] Rafiee K, Feng Q, Coit DW. Condition-based maintenance for repairable deteriorating systems subject to a generalized mixed shock model. *IEEE Trans Reliab* 2015;64:1164–74.
 - [27] Tseng S-T, Tang J. Optimal burn-in time for highly reliable products. *Int J Ind Eng* 2001;8:329–38.
 - [28] Tseng S-T, Peng CY. Optimal burn-in policy by using an integrated Wiener process. *IIE Trans* 2004;36:1161–70.
 - [29] Tsai C-C, Tseng S-T, Balakrishnan N. Optimal burn-in policy for highly reliable products using gamma degradation process. *IEEE Trans Reliab* 2011;60:234–45.
 - [30] Xiang Y, Coit DW, Feng Q. n Subpopulations experiencing stochastic degradation: reliability modeling, burn-in, and preventive replacement. *IIE Trans* 2013;45:391–408.
 - [31] Ye Z-S, Shen Y, Xie M. Degradation-based burn-in with preventive maintenance. *Eur J Oper Res* 2012;221:360–7.
 - [32] Peng H, Feng Q, Coit DW. Simultaneous quality and reliability optimization for microengines subject to degradation. *IEEE Trans Reliab* 2009;58:98–105.
 - [33] Peng Q, Peng H, Coit DW. A degradation-based model for joint optimization of burn-in, quality inspection, and maintenance: a light display device application. *Int J Adv Manuf Technol* 2010;50:801–8.
 - [34] Zhai Q, Ye Z-S, Yang J, Zhao Y. Measurement errors in degradation-based burn-in. *Reliab Eng Syst Saf* 2016;150:126–35.
 - [35] Park JI, Bae SJ. Direct prediction methods on lifetime distribution of organic light-emitting diodes from accelerated degradation tests. *IEEE Trans Reliab* 2010;59:74–90.
 - [36] Park JI, Baek SH, Jeong MK, Bae SJ. Dual features functional support vector machines for fault detection of rechargeable batteries. *IEEE Trans Syst Man Cybern Part C: Appl Rev* 2009;39:480–5.
 - [37] Bae SJ, Kim S-J, Um S-K, Park J-Y, Lee J-H, Cho H. A prediction model of degradation rate for membrane electrode assemblies in direct methanol fuel cells. *Int J Hydrog Energy* 2009;34:5749–58.
 - [38] Bae SJ, Kvam PH. A change-point analysis for modeling incomplete burn-in for light displays. *IIE Trans* 2006;38:489–98.
 - [39] Bae SJ, Yuan T, Ning SN, Kuo W. A Bayesian approach to modeling two-phase degradation using change-point regression. *Reliab Eng Syst Saf* 2015;134:66–74.
 - [40] Muller P, Parmigiani G. Optimal design via curve fitting of Monte Carlo experiments. *J Am Stat Assoc* 1995;90:1322–30.
 - [41] Congdon P. *Applied Bayesian modeling*. Chichester, UK: Wiley; 2003.
 - [42] Barnard J, McCulloch R, Meng XL. Modeling covariance matrices in terms of standard deviations and correlations, with application to shrinkage. *Stat Sin* 2000;10:1281–311.
 - [43] Lunn DJ, Thomas A, Best N, Spiegelhalter D. WinBUGS—a Bayesian modelling framework: concepts, structure, and extensibility. *Stat Comput* 2000;10:325–37.
 - [44] Lu CJ, Meeker WQ. Using degradation measures to estimate a time-to-failure distribution. *Technometrics* 1993;35:161–74.